

Nonmesonic weak decay of double- Λ hypernuclei: A microscopic approach

E. Bauer,¹ G. Garbarino,² and C. A. Rodríguez Peña³

¹*Facultad de Ciencias Astronómicas y Geofísicas, Universidad Nacional de La Plata and IFLP, CONICET C. C. 67, 1900 La Plata, Argentina*

²*IIS G. Peano, I-10147 Torino, Italy*

³*Departamento de Física, Universidad Nacional de La Plata, C. C. 67, 1900 La Plata, Argentina*

(Received 18 March 2015; revised manuscript received 23 May 2015; published 2 July 2015)

The nonmesonic weak decay of double- Λ hypernuclei is studied within a microscopic diagrammatic approach. In addition to the nucleon-induced mechanism, $\Lambda N \rightarrow nN$ and $\Lambda NN \rightarrow nNN$, widely studied in single- Λ hypernuclei, additional hyperon-induced mechanisms, $\Lambda\Lambda \rightarrow \Lambda n$, $\Lambda\Lambda \rightarrow \Sigma^0 n$, and $\Lambda\Lambda \rightarrow \Sigma^- p$, are accessible in double- Λ hypernuclei and are investigated here. As in previous works on single- Λ hypernuclei, we adopt a nuclear matter formalism extended to finite nuclei via the local density approximation and a one-meson exchange weak transition potential (including the ground-state pseudoscalar and vector octets mesons) supplemented by correlated and uncorrelated two-pion-exchange contributions. The weak decay rates are evaluated for hypernuclei in the region of the experimentally accessible light hypernuclei ${}_{\Lambda\Lambda}^{10}\text{Be}$ and ${}_{\Lambda\Lambda}^{13}\text{B}$. Our predictions are compared with a few previous evaluations. The rate for the $\Lambda\Lambda \rightarrow \Lambda n$ decay is dominated by K^- , K^{*-} , and η -exchange and turns out to be about 2.5% of the free Λ decay rate, $\Gamma_{\Lambda}^{\text{free}}$, while the total rate for the $\Lambda\Lambda \rightarrow \Sigma^0 n$ and $\Lambda\Lambda \rightarrow \Sigma^- p$ decays, dominated by π -exchange, amounts to about 0.25% of $\Gamma_{\Lambda}^{\text{free}}$. The experimental measurement of these decays would be essential for the beginning of a systematic study of the nonmesonic decay of strangeness -2 hypernuclei. This field of research could also shed light on the possible existence and nature of the H dibaryon.

DOI: [10.1103/PhysRevC.92.014301](https://doi.org/10.1103/PhysRevC.92.014301)

PACS number(s): 21.80.+a, 25.80.Pw

I. INTRODUCTION

Strangeness nuclear physics plays an important role in modern nuclear and hadronic physics and involves important connections with astrophysical processes and observables as well as with quantum chromodynamics (QCD). In particular, the weak decay of Λ hypernuclei is the only actual source of information on strangeness-changing four-baryon weak interactions. A great variety of theoretical and experimental studies were performed on the decay of such systems. Let us mention the experimental and theoretical analysis of nucleon-coincidence emission spectra and the theoretical modeling of the decay channels within complete one-meson-exchange weak transition potentials, which in some cases have been supplemented by a two-pion-exchange mechanism. A reasonable agreement between data and predictions have been reached for the mesonic and nonmesonic decay rates, the Γ_n/Γ_p ratio between the neutron- and the proton-induced decay widths, the $\Gamma_2/\Gamma_{\text{NM}}$ ratio between the two-nucleon induced and the total nonmesonic rates, and the intrinsic asymmetry parameter a_{Λ} for the decay of polarized hypernuclei [1]. Nevertheless, discrepancies between theory and experiment are still present for the emission spectra involving protons [2–4].

Despite their implications on the possible existence of dibaryon states and multistrangeness hypernuclei and on the study of compact stars, much less is known on strangeness -2 hypernuclei. Little information is available on cascade hypernuclei, for instance, on the Ξ -nucleus potential. The existence of the strong $\Xi^- p \rightarrow \Lambda\Lambda$ reaction makes Ξ hypernuclei unstable with respect to the strong interaction. However, this conversion reaction can be exploited to produce double- Λ hypernuclei.

Investigations on the structure of double- Λ hypernuclei are important to determine the $\Lambda\Lambda$ strong interaction, which

is poorly known at present. Indeed, only a few double- Λ hypernuclei events have been studied experimentally up to date. In the KEK-176 and KEK-373 experiments, ${}_{\Lambda\Lambda}^4\text{H}$, ${}_{\Lambda\Lambda}^6\text{He}$, and ${}_{\Lambda\Lambda}^{10}\text{Be}$ have been identified, while less unambiguous events were recorded for ${}_{\Lambda\Lambda}^6\text{He}$ and ${}_{\Lambda\Lambda}^{10}\text{Be}$ in the 1960s and for ${}_{\Lambda\Lambda}^{13}\text{B}$ in the early 1990s [5]. The observation of the so-called NAGARA event implies a weak and attractive $\Lambda\Lambda$ interaction, i.e., a bond energy $\Delta B_{\Lambda\Lambda}({}_{\Lambda\Lambda}^6\text{He}) \equiv B_{\Lambda\Lambda}({}_{\Lambda\Lambda}^6\text{He}) - 2B_{\Lambda}({}_{\Lambda}^5\text{He}) = (0.67 \pm 0.17) \text{ MeV}$ [6]. In [7] the authors demonstrated that this bond energy value, which will be employed in the present work as the binding energy between the two Λ 's, describes well double- Λ hypernuclear data in the mass range from 6 to 13. Future experiments on strangeness -2 hypernuclei will be carried out at J-PARC [8] and FAIR (PANDA Collaboration) [9]. In particular, we mention that the J-PARC E07 experiment, adopting the production reaction $p(K^-, K^+)\Xi^-$ and a diamond target, is based on a newly established hybrid-emulsion method, with 10 times better statistics of the previous KEK-E373 experiment. We also note that the PANDA experiment at FAIR will use antiproton-induced reactions, $\bar{p}p \rightarrow \Xi\Xi$, and that a variety of hypernuclei will be accessible by using a ${}^{12}\text{C}$ primary target, ranging from ${}_{\Lambda\Lambda}^7\text{Li}$ to ${}_{\Lambda\Lambda}^{12}\text{B}$.

On the weak interaction side, double- Λ hypernuclei offer the opportunity to access the following Λ -induced Λ decay channels: $\Lambda\Lambda \rightarrow \Lambda n$, $\Lambda\Lambda \rightarrow \Sigma^- p$, $\Lambda\Lambda \rightarrow \Sigma^0 n$ (with a $|\Delta S| = 1$ change in strangeness) and $\Lambda\Lambda \rightarrow nn$ ($|\Delta S| = 2$). Antisymmetry constraints on the $\Lambda\Lambda$ initial state restrict the pair to be coupled to $S = 0$ and $J = 0$, thus only two nonmesonic decay channels are accessible: ${}^1S_0 \rightarrow {}^1S_0$ and ${}^1S_0 \rightarrow {}^3P_0$ in spectroscopic notation. No data are available on these decays, apart from the claim for the observation of a single event at KEK [10]. The experimental signature of a $\Lambda\Lambda \rightarrow \Lambda n$ decay is clear, i.e., the emission of a large momentum Λ ($\sim 425 \text{ MeV}$), but the major problem

is that these events are expected to be somewhat rare. The usual neutron- and proton-induced decays, $\Lambda n \rightarrow nn$ and $\Lambda p \rightarrow np$, dominate over the Λ -induced ones in double- Λ hypernuclei.

Realistic calculation and improved measurements of the Λ -induced Λ weak decays could also provide hints on the possible existence of the long-hunted H dibaryon, predicted long ago by Jaffe [11]. A reliable calculation is important in the design of future experiments at J-PARC and FAIR, where these weak processes could be unambiguously observed for the first time.

Only a few predictions are available for such interesting strangeness-changing processes [12–14]; unfortunately, there are major disagreements among the predictions of these works, which adopted different frameworks. Their results are discussed in the following together with the new ones obtained here.

In this paper we present a microscopic calculation of both the Λ - and nucleon-induced Λ decay rates for double- Λ hypernuclei by using a nuclear matter formalism; both one- and two-nucleon stimulated processes, $\Lambda N \rightarrow nN$ and $\Lambda NN \rightarrow nNN$, are taken into account, while the $\Lambda\Lambda \rightarrow nn$ decay channel is not considered here because, requiring a change in strangeness of two units, it is much less likely than the other Λ -induced processes. Results for finite hypernuclei in the mass range of the empirically interesting ${}^{10}_{\Lambda\Lambda}\text{Be}$ and ${}^{13}_{\Lambda\Lambda}\text{B}$ systems are reported within the local density approximation. The same microscopic approach showed that Pauli exchange and ground-state correlation contributions are very important for a detailed calculation of the rates, the asymmetry parameter, and the nucleon emission spectra in the nonmesonic weak decay of Λ hypernuclei [3,15–17]. Less pronounced effects have been reported by including the Δ -baryon resonance in the microscopic approach [4].

The paper is organized as follows. In Sec. II we present the theoretical formalism employed for the evaluation of the decay rates, while in Sec. III we discuss the adopted weak potential model. In Sec. IV the numerical results are discussed and compared with previous calculations. Finally, in Sec. V we draw our conclusions.

II. FORMALISM

Let us start by writing the total nonmesonic decay rate for a double- Λ hypernucleus as

$$\Gamma_{\text{NM}} = \Gamma_{\text{N}} + \Gamma_{\Lambda}, \quad (1)$$

where

$$\begin{aligned} \Gamma_{\text{N}} &= \Gamma(\Lambda n \rightarrow nn) + \Gamma(\Lambda p \rightarrow np) + \Gamma(\Lambda NN \rightarrow nNN) \\ &= \Gamma_n + \Gamma_p + \Gamma_2 \\ &= \Gamma_1 + \Gamma_2, \\ \Gamma_{\Lambda} &= \Gamma(\Lambda\Lambda \rightarrow \Lambda n) + \Gamma(\Lambda\Lambda \rightarrow \Sigma^0 n) + \Gamma(\Lambda\Lambda \rightarrow \Sigma^- p) \\ &= \Gamma_{\Lambda n} + \Gamma_{\Sigma^0 n} + \Gamma_{\Sigma^- p}, \end{aligned} \quad (2)$$

are the total nucleon- and Λ -induced decay rates, respectively. Note that the two-nucleon-induced rate reads $\Gamma_2 = \Gamma(\Lambda NN \rightarrow nNN) = \Gamma(\Lambda nn \rightarrow$

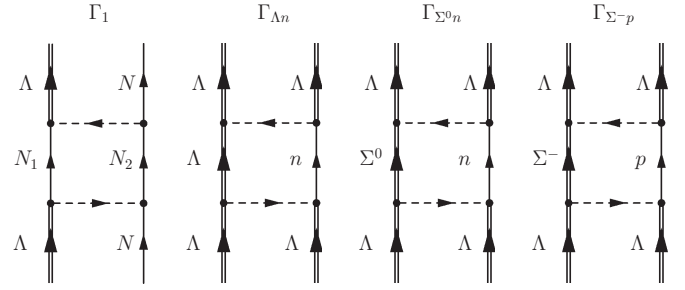


FIG. 1. Goldstone diagrams for the evaluation of the $\Lambda N \rightarrow nN$, $\Lambda\Lambda \rightarrow \Lambda n$, $\Lambda\Lambda \rightarrow \Sigma^0 n$, and $\Lambda\Lambda \rightarrow \Sigma^- p$ decay rates in infinite nuclear matter.

$nnn) + \Gamma(\Lambda np \rightarrow nnp) + \Gamma(\Lambda pp \rightarrow npp)$, while the definitions of the partial rates Γ_n , Γ_p , $\Gamma_{\Lambda n}$, $\Gamma_{\Sigma^0 n}$, and $\Gamma_{\Sigma^- p}$ are self-explanatory.

As in previous papers on Λ hypernuclei, we adopt a microscopic formalism. In this many-body technique the calculation is performed in infinite nuclear matter and then it is extended to finite nuclei through the local density approximation (LDA) [18].

The many-body contributions we consider for describing the $\Lambda N \rightarrow nN$ and $\Lambda\Lambda \rightarrow YN$ processes in nuclear matter are given by the Goldstone diagrams of Fig. 1. They provide the various decay widths through the relations: $\Gamma_f^{\Lambda N} = -2 \text{Im} \Sigma_f^{\Lambda N}$, $\Sigma_f^{\Lambda N}$ being the ΛN self-energy and $f = nn$ and np denoting the possible final states; $\Gamma_f^{\Lambda\Lambda} = -2 \text{Im} \Sigma_f^{\Lambda\Lambda}$, $\Sigma_f^{\Lambda\Lambda}$ being the $\Lambda\Lambda$ self-energy and $f = \Lambda n, \Sigma^0 n$ and $\Sigma^- p$ denoting the possible final states.

Let us consider infinite nuclear matter with Fermi momentum k_F and denote the four-momenta of the initial Λ 's with $k = (k_0, \mathbf{k})$ and $k' = (k'_0, \mathbf{k}')$ and the four-momenta of the final particles by $p_1 = (p_{10}, \mathbf{p}_1)$ (hyperon) and $p_2 = (p_{20}, \mathbf{p}_2)$ (nucleon). In a schematic way, for the Goldstone diagrams of Fig. 1 one obtains the partial decay width to the YN ($= \Lambda n, \Sigma^0 n$ and $\Sigma^- p$) final state as follows:

$$\Gamma_{YN}(\mathbf{k}, k_F) = \sum_f |\langle f | V^{\Lambda\Lambda \rightarrow YN} | 0 \rangle_{k_F}|^2 \delta(E_f - E_0), \quad (3)$$

where $V^{\Lambda\Lambda \rightarrow YN}$ is the weak transition potential, $|0\rangle_{k_F}$ denotes the initial state with energy E_0 including the nuclear matter ground state and the two Λ 's in the $1s$ level, and $|f\rangle$ the possible final states with energy E_f including nuclear matter and the YN pair. Note also that momentum conservation, i.e., $\mathbf{k}' = \mathbf{p}_1 + \mathbf{p}_2 - \mathbf{k}$, implies that only one of the initial momenta (\mathbf{k}) is an independent variable once \mathbf{p}_1 and \mathbf{p}_2 are integrated out, as in Eq. (3). We remind the reader that, as anticipated, the decay rates of Eq. (3) are obtained as the imaginary part of the corresponding self-energies of Fig. 1. Self-energy diagrams provide cut graphs representing the decay rates: Each one of the Goldstone diagrams in Fig. 1 is cut by a horizontal line at the intermediate baryon-baryon state to provide the decay rate; in this rate the baryons which are crossed by the cut line appear as final on-shell particles. Explicit expressions for the self-energies and decay rates obtained from the diagrams of Fig. 1 are given below.

The decay rates for a finite hypernucleus are obtained from the previous partial widths via the LDA:

$$\Gamma_{YN} = \int d\mathbf{k} |\tilde{\psi}_\Lambda(\mathbf{k})|^2 \int d\mathbf{r} |\psi_\Lambda(\mathbf{r})|^2 \Gamma_{YN}(\mathbf{k}, k_F(r)). \quad (4)$$

This approximation (see Appendix A) consists of introducing a local nucleon Fermi momentum $k_F(r) = \{3\pi^2\rho(r)/2\}^{1/3}$ in terms of the density profile $\rho(r)$ of the nuclear core and then in averaging the partial widths over the nuclear volume. This average is weighted by the probability per unit volume of finding the Λ which then transforms into the final nucleon at a given position \mathbf{r} , $|\psi_\Lambda(\mathbf{r})|^2$. A further average is performed over the momentum distributions of the Λ , $\tilde{\psi}_\Lambda(\mathbf{k})$ (both initial Λ 's lie in the $1s_{1/2}$ single-particle state). The calculation is performed for double- Λ hypernuclei with mass number $A = 10$ –13 to mimic the behavior of the experimentally accessible finite hypernuclei ${}^{10}_{\Lambda\Lambda}\text{Be}$ and ${}^{13}_{\Lambda\Lambda}\text{B}$. As in [12], for the function $\psi_\Lambda(\mathbf{r})$ we use a $1s_{1/2}$ harmonic oscillator wave function; its frequency $\hbar\omega = 13.6$ MeV is obtained from the fit of [19] of the experimental binding energies of ${}^6_{\Lambda\Lambda}\text{He}$, ${}^{10}_{\Lambda\Lambda}\text{Be}$, and ${}^{13}_{\Lambda\Lambda}\text{B}$. The energies of the initial Λ with momentum \mathbf{k} is given by $k_0 = m_\Lambda + \mathbf{k}^2/(2m_\Lambda) + V_\Lambda$, where for the binding term we adopt the value $V_\Lambda = -\hbar\omega = -13.6$ MeV.

Analyses of Σ formation spectra in the (K^-, π^\pm) and (π^+, K^+) reactions showed that the Σ -nucleus potential has a substantial isospin dependence and, with the exception of very light systems (the only quasibound state of a Σ in a nucleus was observed in ${}^4_\Sigma\text{He}$), is repulsive: $V_\Sigma \sim +(10\text{--}50)$ MeV at normal nuclear density. In the present calculation we adopt the value $V_\Sigma = +30$ MeV.

Before we give explicit expressions for the decay widths in nuclear matter, it is convenient to show the general form of the weak transition potential. The standard weak, strangeness-changing transition potential for the $\Lambda\Lambda \rightarrow YN$ processes can be written as

$$V^{\Lambda\Lambda \rightarrow YN}(q) = \sum_{\tau=0,1} O_\tau V_\tau(q), \quad O_\tau = \begin{cases} 1 & \text{for } \tau = 0 \\ \boldsymbol{\tau}_1 \cdot \boldsymbol{\tau}_2 & \text{for } \tau = 1 \end{cases}, \quad (5)$$

where

$$\begin{aligned} V_\tau(q) = & (G_F m_\pi^2) \{ S_\tau(q) \boldsymbol{\sigma}_1 \cdot \hat{\mathbf{q}} + S'_\tau(q) \boldsymbol{\sigma}_2 \cdot \hat{\mathbf{q}} \\ & + P_{L,\tau}(q) \boldsymbol{\sigma}_1 \cdot \hat{\mathbf{q}} \boldsymbol{\sigma}_2 \cdot \hat{\mathbf{q}} \\ & + P_{C,\tau}(q) + P_{T,\tau}(q) (\boldsymbol{\sigma}_1 \times \hat{\mathbf{q}}) \cdot (\boldsymbol{\sigma}_2 \times \hat{\mathbf{q}}) \\ & + i S_{V,\tau}(q) (\boldsymbol{\sigma}_1 \times \boldsymbol{\sigma}_2) \cdot \hat{\mathbf{q}} \}. \end{aligned} \quad (6)$$

In these equations the spin-isospin dependence is shown explicitly, while the momentum dependence is given by the functions $S_\tau(q)$, $S'_\tau(q)$, $P_{L,\tau}(q)$, $P_{C,\tau}(q)$, $P_{T,\tau}(q)$, and $S_{V,\tau}(q)$. We return to these functions in the next section.

To enforce antisymmetrization, for each one of the contributions of Fig. 1 we also consider the corresponding exchange

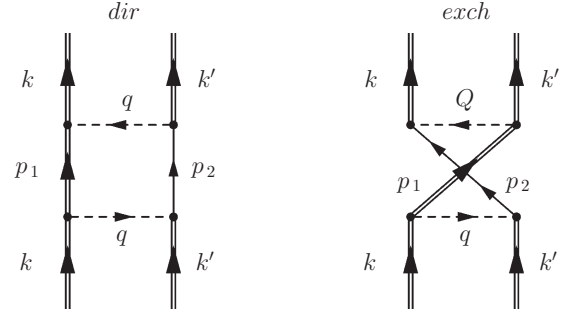


FIG. 2. Direct and exchange Goldstone diagrams for the $\Lambda\Lambda \rightarrow \Lambda n$ decay.

contribution. In Fig. 2 we give the direct and exchange diagrams for $\Lambda\Lambda \rightarrow \Lambda n$.

Through the standard rules for Goldstone diagrams one writes down the explicit expression for these contributions. In particular, for $\Gamma_{\Lambda n} = -2 \text{Im} \Sigma_{\Lambda n}$ we have

$$\begin{aligned} \Gamma_{\Lambda n}(\mathbf{k}, k_F) &= -2 \text{Im} \int \frac{d^4 p_1}{(2\pi)^4} \int \frac{d^4 p_2}{(2\pi)^4} G_\Lambda(p_1) G_n(p_2) \frac{1}{4} \\ &\times \sum_{\text{all spins}} \langle \gamma_\Lambda(k) \gamma_\Lambda(k') | (V^{\Lambda\Lambda \rightarrow \Lambda n})^\dagger | \gamma_\Lambda(p_1) \gamma_n(p_2) \rangle_{\text{ant}} \\ &\times \langle \gamma_\Lambda(p_1) \gamma_n(p_2) | V^{\Lambda\Lambda \rightarrow \Lambda n} | \gamma_\Lambda(k) \gamma_\Lambda(k') \rangle_{\text{ant}}, \end{aligned} \quad (7)$$

where with $\gamma_{B(K)}$ we represent the spin, isospin, and energy-momentum K of the baryon B . Explicit expressions for the hyperon and neutron propagators $G_\Lambda(p)$ and $G_n(p)$ are given in Appendix C. After performing the summation over spin, the evaluation of the isospin matrix element and the energy integration, one obtains the antisymmetrized decay rate:

$$\begin{aligned} \Gamma_{\Lambda n}(\mathbf{k}, k_F) = & \pi (G_F m_\pi^2)^2 \int \frac{d^3 p_1}{(2\pi)^3} \int \frac{d^3 p_2}{(2\pi)^3} (2 \mathcal{W}_0^{\text{dir}}(q) \\ & - \mathcal{W}_0^{\text{exch}}(q, \mathcal{Q}) \theta(|\mathbf{p}_2| - k_F) \\ & \times \delta(k_0 + k'_0 - E_\Lambda(p_1) - E_n(p_2))), \end{aligned} \quad (8)$$

where E_Λ (E_n) is the total Λ (neutron) energy, while $q = k - p_1$ and $\mathcal{Q} = k - p_2$. For the direct term, the momentum matrix element of the interaction turns out to be

$$\begin{aligned} \mathcal{W}_0^{\text{dir}}(q) = & \{ S_0^2(q) + S_0'^2(q) + P_{L,0}^2(q) + P_{C,0}^2(q) \\ & + 2 P_{T,0}^2(q) + 2 S_{V,0}^2(q) \}, \end{aligned} \quad (9)$$

while for the exchange term we have

$$\begin{aligned} \mathcal{W}_0^{\text{exch}}(q, \mathcal{Q}) &= (\hat{\mathbf{q}} \cdot \hat{\mathcal{Q}}) \mathcal{S}_0(q, \mathcal{Q}) + (2(\hat{\mathbf{q}} \cdot \hat{\mathcal{Q}})^2 - 1) P_{L,0}(q) P_{L,0}(\mathcal{Q}) \\ &+ 2((\hat{\mathbf{q}} \cdot \hat{\mathcal{Q}})^2 - 1) P_{T,0}(q) P_{T,0}(\mathcal{Q}) \\ &- 2(\hat{\mathbf{q}} \cdot \hat{\mathcal{Q}})^2 (P_{L,0}(q) P_{T,0}(\mathcal{Q}) + P_{L,0}(\mathcal{Q}) P_{T,0}(q)) \\ &+ P_{C,0}(q) P_{C,0}(\mathcal{Q}) + P_{C,0}(q) P_{L,0}(\mathcal{Q}) + P_{C,0}(\mathcal{Q}) P_{L,0}(q) \\ &+ 2(P_{C,0}(q) P_{T,0}(\mathcal{Q}) + P_{C,0}(\mathcal{Q}) P_{T,0}(q)), \end{aligned} \quad (10)$$

where we have defined

$$\begin{aligned} S_0(q, Q) = & (S_0(q) + S'_0(q))(S_0(Q) + S'_0(Q)) \\ & - 2(S_0(q)S_{V,0}(Q) + S_{V,0}(q)S_0(Q)) \\ & + 2(S'_0(q)S_{V,0}(Q) + S_{V,0}(q)S'_0(Q)). \end{aligned} \quad (11)$$

Note from Eqs. (9)–(11) that, being the $\Lambda\Lambda \rightarrow \Lambda n$ weak potential of isoscalar nature, we have fixed $\tau = 0$ in Eqs. (5) and (6). In Appendix C we present explicit expressions for the $\Lambda\Lambda \rightarrow \Sigma^0 n$ and $\Lambda\Lambda \rightarrow \Sigma^- p$ decay rates.

III. THE POTENTIAL MODEL

We adopt a meson-exchange description of the weak transition potential including π , η , K , ρ , ω , and K^* mesons (these contribute to the one-meson-exchange part, denoted by OME in the following) together with a two-pion-exchange mechanism (TPE) consisting of both an uncorrelated and a correlated part. The explicit expressions for the OME potentials are given in Appendix B. The OME contribution to the momentum-dependent functions S_τ , S'_τ , $P_{L,\tau}$, $P_{C,\tau}$, $P_{T,\tau}$, and $S_{V,\tau}$ appearing in Eq. (6) and in Eqs. (9)–(11), include short-range correlations and vertex form factors and are obtained from Appendix B of [20] once the modifications concerning the baryon coupling constants discussed in Appendix B of the present paper are implemented.

Because isospin is conserved in the strong baryon vertices, the $\Lambda\Lambda \rightarrow \Lambda n$ decay process has isoscalar character [$\tau = 0$, in Eq. (5)] and only η , K , ω , and K^* exchange together with TPE contribute; instead, the $\Lambda\Lambda \rightarrow \Sigma^0 n$ and the $\Lambda\Lambda \rightarrow \Sigma^- p$ processes are of isovector nature [$\tau = 1$, in Eq. (5)] and the contributing mesons are π , K , ρ , and K^* . We again refer to Appendix B for details. At the OME level one naively expects the $\Lambda\Lambda \rightarrow \Lambda n$ decay ($\Lambda\Lambda \rightarrow \Sigma^- p$, $\Lambda\Lambda \rightarrow \Sigma^0 n$ decays) to be dominated by K exchange (π exchange). In particular, from the $\Lambda\Lambda \rightarrow \Lambda n$ ($\Lambda\Lambda \rightarrow \Sigma^0 n$) channel one could obtain information on the $\Lambda\Lambda K$ ($\Lambda\Sigma K$) vertex; these vertices are important to constrain $SU(3)$ chiral perturbation theory [12].

As in [21], the TPE for the $\Lambda N \rightarrow nN$ processes is taken from [22], where in particular a chiral unitary model was used to account for the correlated two-pion exchange in the scalar-isoscalar channel. For the $\Lambda\Lambda \rightarrow YN$ processes, the two-pion-exchange contributions are obtained from the $\Lambda N \rightarrow \Lambda N$ scalar-isoscalar two-pion-exchange strong interaction potential derived in [23], again by a chiral unitary approach. The present work is the first one to include the TPE mechanism in the $\Lambda\Lambda \rightarrow YN$ nonmesonic decays, while we note that the calculations of [17,21,22,24] have included the TPE mechanism in $\Lambda n \rightarrow nN$ nonmesonic decay calculations.

We assume the $\Delta I = 1/2$ rule on the isospin change to be valid for all baryon-baryon-meson weak vertices, although it is phenomenologically justified only for the $\Lambda N\pi$ free vertex. By further neglecting the small mass difference between Σ^0 and Σ^- one obtains that the rates for decays into $\Sigma^0 n$ and $\Sigma^- p$ states are simply related by

$$\frac{\Gamma_{\Sigma^- p}}{\Gamma_{\Sigma^0 n}} = 2, \quad (12)$$

and it is sufficient to calculate the decay rates $\Gamma_{\Lambda n}$ and $\Gamma_{\Sigma^0 n}$.

IV. RESULTS

The calculations refer to the mass range corresponding to the experimentally accessible $^{10}_{\Lambda\Lambda}\text{Be}$ and $^{13}_{\Lambda\Lambda}\text{B}$ hypernuclei. Practically, the calculations are performed with a mass number $A = N + Z + 2 = 12$ and an equal number of neutrons and protons, $N = Z = 5$. We verified that the numerical results do not change appreciably by changing A by one or two units: We will refer to them as the results for $A \sim 12$ double- Λ hypernuclei.

In Table I we give our results for the $\Lambda\Lambda \rightarrow \Lambda n$, $\Lambda\Lambda \rightarrow \Sigma^0 n$, and $\Lambda\Lambda \rightarrow \Sigma^- p$ weak decay widths. Predictions are given for the individual meson exchanges and for the most relevant combinations among them. The results for $\Gamma_{\Sigma^- p}$ are obtained as $\Gamma_{\Sigma^- p} = 2\Gamma_{\Sigma^0 n}$ because the $\Delta I = 1/2$ isospin rule is assumed here. As anticipated, the rate $\Gamma_{\Lambda n}$ ($\Gamma_{\Sigma^0 n}$) has no contribution from isovector (isoscalar) mesons.

In the OME sector the rate $\Gamma_{\Lambda n}$ receives major contributions by K^- and K^{*-} exchange. The η contribution is smaller but non-negligible. Instead, both the ω exchange and the TPE contributions are negligible; the TPE provides the smallest contribution. The addition of K and K^* exchange provides a decay rate which is about 65% larger than the complete result for $\Gamma_{\Lambda n}$ because of a constructive interference between the two meson contributions. However, the further addition of the η meson, from a destructive interference, lowers the decay rate to be only 4% larger than the complete result.

The rates $\Gamma_{\Sigma^0 n}$ and $\Gamma_{\Sigma^- p}$ are much smaller than $\Gamma_{\Lambda n}$ and, as expected, are dominated by π exchange. Much smaller single contributions originate from K , K^* , and ρ exchange. However, the combined effect of these mesons is to increase the rates by about 20% thanks to constructive interference effects. From the kinematics point of view, mesons heavier than the pion are expected to contribute less to the rates $\Gamma_{\Sigma^0 n}$ and $\Gamma_{\Sigma^- p}$ than to the rate $\Gamma_{\Lambda n}$ because the $\Lambda\Lambda \rightarrow \Lambda n$ process is characterized by larger momentum transfers than the $\Lambda\Lambda \rightarrow \Sigma^0 n$ and $\Lambda\Lambda \rightarrow \Sigma^- p$ processes. This is confirmed by the results of Table I: The $\Gamma_{\Lambda n}$ rate receives substantial contributions from K , K^* , and η exchange, while $\Gamma_{\Sigma^0 n}$ is dominated by π exchange.

TABLE I. Results for the $\Lambda\Lambda \rightarrow \Lambda n$, $\Lambda\Lambda \rightarrow \Sigma^0 n$, and $\Lambda\Lambda \rightarrow \Sigma^- p$ weak decay widths in $A \sim 12$ double- Λ hypernuclei are given as a percentage of the free Λ decay rate. Predictions are given for the individual contributing mesons and for the most relevant meson combinations.

Model	$\Gamma_{\Lambda n}$	$\Gamma_{\Sigma^0 n}$	$\Gamma_{\Sigma^- p}$
π	–	0.070	0.140
K	1.73	0.001	0.002
η	0.35	–	–
ρ	–	0.001	0.002
K^*	0.84	0.002	0.004
ω	0.01	–	–
TPE	0.002	–	–
$\pi + K + K^*$	4.14	0.081	0.162
$\pi + K + K^* + \eta$	2.57	0.081	0.162
All	2.48	0.084	0.168

TABLE II. Predictions for the one-nucleon-induced nonmesonic weak decay rates for $A \sim 12$ double- Λ hypernuclei. The results of the present work are given together with previous ones available for ${}^6_{\Lambda\Lambda}\text{He}$ [12,13]. The decay rates are in units of the free Λ decay width.

Model and Ref.	Γ_n	Γ_p	Γ_n/Γ_p	$\Gamma_1 = \Gamma_n + \Gamma_p$
This work ($A \sim 12$)	0.48	1.12	0.43	1.60
OME (${}^6_{\Lambda\Lambda}\text{He}$) [12]	0.30	0.66	0.46	0.96
$\pi + 2\pi/\rho + 2\pi/\sigma$ (${}^6_{\Lambda\Lambda}\text{He}$) [13]	0.295	0.441	0.669	0.736

Before comparing the above predictions with those obtained in previous calculations, in Table II we present our results for the one-nucleon-induced nonmesonic decay rates together with determinations from [12,13]. Our predictions for Γ_n and Γ_p in $A \sim 12$ double- Λ hypernuclei are larger than previously obtained for ${}^6_{\Lambda\Lambda}\text{He}$; indeed, it is well established that, in single- Λ hypernuclei, the values of the $\Lambda N \rightarrow nN$ rates are increasing as a function of A and saturate for $A \sim 20$. One expects the neutron- and proton-induced rates for a double- Λ hypernucleus to be larger than twice the corresponding rates for a single- Λ hypernucleus with one unit less mass number: $\Gamma_1({}^A_{\Lambda\Lambda}Z) > 2\Gamma_1({}^{A-1}_{\Lambda}Z)$. Apart from the fact that a double- Λ hypernucleus has twice the number of Λ 's than a single- Λ hypernucleus, one has to consider that the binding energy of a Λ is larger in ${}^A_{\Lambda\Lambda}Z$ than in ${}^{A-1}_{\Lambda}Z$. This is well confirmed experimentally by binding data on ${}^6_{\Lambda\Lambda}\text{He}$ and ${}^5_{\Lambda}\text{He}$. The same behavior is expected in our mass range [25], although for increasing A the Λ binding energies for double- Λ and single- Λ hypernuclei should converge towards a common value. Our results confirm the described behavior: The one-nucleon-induced nonmesonic decay rate obtained for an $A = 12$ double- Λ hypernucleus, $\Gamma_1 = 1.60\Gamma_{\Lambda}^{\text{free}}$, is about 5% larger than twice the same rate we obtain within the same framework and weak potential model for ${}^{11}_{\Lambda}\text{B}$, $\Gamma_1({}^{11}_{\Lambda}\text{B}) = 0.76\Gamma_{\Lambda}^{\text{free}}$. To conclude the discussion of the nucleon-induced nonmesonic decay, we come to the decay rate Γ_2 for the two-nucleon-induced processes, $\Lambda NN \rightarrow nNN$ (with $N = n$ or p). We obtained $\Gamma_2 = 0.72\Gamma_{\Lambda}^{\text{free}}$ and thus $\Gamma_2 = 0.31\Gamma_N$. This result is not included in Table II because the determinations by other authors therein displayed do not contain this decay channel. Similarly to the one-nucleon-induced case, for the two-nucleon-induced rate the inequality $\Gamma_2({}^A_{\Lambda\Lambda}Z) > 2\Gamma_2({}^{A-1}_{\Lambda}Z)$ turns out to be satisfied: Indeed, within the same framework and weak potential model we find $\Gamma_2({}^{11}_{\Lambda}\text{B}) = 0.27\Gamma_{\Lambda}^{\text{free}}$. The difference between the two-nucleon-induced decay rate for an $A = 12$ double- Λ hypernucleus and twice the rate $\Gamma_2({}^{11}_{\Lambda}\text{B})$ is about 25%. The main contribution to this difference is from the sensitivity of the rate Γ_2 to the hypernucleus mass number and not to the Λ binding energy.

In Table III our final results for the $\Lambda\Lambda \rightarrow \Lambda n$, $\Lambda\Lambda \rightarrow \Sigma^0 n$, and $\Lambda\Lambda \rightarrow \Sigma^- p$ decay rates in $A \sim 12$ double- Λ hypernuclei are given together with existing calculations for ${}^6_{\Lambda\Lambda}\text{He}$ and ${}^{10}_{\Lambda\Lambda}\text{Be}$ [12–14].

Our calculation is easily comparable with the finite nucleus (single-particle shell model) OME calculation of [12] because TPE turned out to give a negligible contribution in the present

TABLE III. Predictions for the $\Lambda\Lambda \rightarrow \Lambda n$, $\Lambda\Lambda \rightarrow \Sigma^0 n$, and $\Lambda\Lambda \rightarrow \Sigma^- p$ weak decay rates for $A \sim 12$ double- Λ hypernuclei of the present work and for ${}^6_{\Lambda\Lambda}\text{He}$ and ${}^{10}_{\Lambda\Lambda}\text{Be}$ from previous works. The decay rates are in units of $10^{-2}\Gamma_{\Lambda}^{\text{free}}$, $\Gamma_{\Lambda}^{\text{free}}$ being the free Λ decay width.

Model and Ref.	$\Gamma_{\Lambda n}$	$\Gamma_{\Sigma^0 n}$	$\Gamma_{\Sigma^- p}$
This work ($A \sim 12$)	2.48	0.08	0.17
OME (${}^6_{\Lambda\Lambda}\text{He}$) [12]	3.6	0.13	0.26
$\pi + K + \omega + 2\pi/\rho + 2\pi/\sigma$ (${}^6_{\Lambda\Lambda}\text{He}$) [13]	5.3	0.10	0.20
$\pi + K + \omega + 2\pi/\rho + 2\pi/\sigma$ (${}^{10}_{\Lambda\Lambda}\text{Be}$) [13]	3.4	0.07	0.13
$\pi + K$ (${}^6_{\Lambda\Lambda}\text{He}$) [14]	0.03	0.51	1.00
$\pi + K + \text{DQ}$ (${}^6_{\Lambda\Lambda}\text{He}$) [14]	0.24	0.65	0.85

calculation and the OME models employed in both works have the same pseudoscalar and vector meson content. Our predictions for $\Gamma_{\Lambda n}$, $\Gamma_{\Sigma^0 n}$, and $\Gamma_{\Sigma^- p}$ are smaller, by 30%–40%, than the ones of the finite nucleus calculation. We think this is mainly because of the fact that in [12] a lighter hypernucleus, ${}^6_{\Lambda\Lambda}\text{He}$, was considered. Indeed, we proved numerically that the Λ -induced Λ decay rate $\Gamma_{\Lambda} = \Gamma_{\Lambda n} + \Gamma_{\Sigma^0 n} + \Gamma_{\Sigma^- p}$ decreases for increasing mass number A : A decrease of 2% in the rate $\Gamma_{\Lambda n}$ is obtained if the calculation is performed with $A = 10$ instead of $A = 12$ (note that our LDA calculation cannot be extended to small mass numbers as $A = 6$). The results of [13] of Table III also corroborates this behavior. Note instead that the one-nucleon-induced Λ decay rate $\Gamma_1 = \Gamma_n + \Gamma_p$ (for both single- and double- Λ hypernuclei) increases with A . The different behavior of Γ_1 and Γ_{Λ} as a function of A is easily explained as follows. On the one hand, the rate Γ_1 increases and then saturates with A because it somehow measures the number of nucleons which can interact with the Λ , i.e., the nucleons which can induce a $\Lambda N \rightarrow nN$ decay. On the other hand, for increasing A the average distance between two Λ 's in a double- Λ hypernucleus increases and thus the rate Γ_{Λ} becomes smaller. Our Λ -induced predictions exhibit a behavior which is similar to the one obtained in [12], which also enforced the $\Delta I = 1/2$ rule: The ratio $\Gamma_{\Lambda n}/\Gamma_{\Sigma^0 n}$ is about 28 in the finite nucleus approach, while in the present work,

$$\frac{\Gamma_{\Lambda n}}{\Gamma_{\Sigma^0 n}} \sim 30. \quad (13)$$

Another ratio between decay rates deserves to be considered: It involves the neutron-induced rate Γ_n and the Λ -induced rate $\Gamma_{\Lambda n}$. One expects the $\Gamma_n/\Gamma_{\Lambda n}$ ratio to be driven by the number of Λn pairs in the hypernucleus, i.e., by the number of neutrons N_n that can induce the nonmesonic decay. In a naive picture, $\Gamma_n/\Gamma_{\Lambda n}$ is thus proportional to N_n . We obtain

$$\frac{\Gamma_n}{\Gamma_{\Lambda n}} \sim 19.4, \quad (14)$$

while in the finite nucleus approach in [12], $\Gamma_n/\Gamma_{\Lambda n} \sim 8.3$. The different results are mainly from the different neutron numbers in the two calculations, $N_n = 5$ in the present calculation and $N_n = 2$ in [12]: Indeed, $(\Gamma_n/\Gamma_{\Lambda n})_{N_n=5}/(\Gamma_n/\Gamma_{\Lambda n})_{N_n=2} \sim 2.3$, while the corresponding ratio between the neutron numbers is $5/2 = 2.5$.

In [13], a phenomenological, correlated two-pion-exchange ($2\pi/\sigma + 2\pi/\rho$) mechanism was added to a $\pi + K + \omega$ -exchange model for a finite nucleus calculation for ${}^6_{\Lambda\Lambda}\text{He}$ and ${}^{10}_{\Lambda\Lambda}\text{Be}$. The authors found an improvement in the calculation of the Γ_n/Γ_p ratio for single- Λ hypernuclei by including the $2\pi/\sigma$ and $2\pi/\rho$ potentials [26] together with K exchange [13]. We note that in [13] the same Λ wave function previously adopted for ${}^5_{\Lambda}\text{He}$ was used for ${}^6_{\Lambda\Lambda}\text{He}$, despite, as explained above, a Λ is more bound in ${}^6_{\Lambda\Lambda}\text{He}$ than in ${}^5_{\Lambda}\text{He}$. This assumption leads to an underestimation of the Γ_n and Γ_p decay rates reported in Table II for ${}^6_{\Lambda\Lambda}\text{He}$. In the same paper, the wave function of ${}^6_{\Lambda\Lambda}\text{He}$ (${}^{10}_{\Lambda\Lambda}\text{Be}$) was described by an $\alpha + \Lambda + \Lambda$ three-body cluster model ($\alpha + \alpha + \Lambda + \Lambda$ four-body cluster model). Although the final results for ${}^{10}_{\Lambda\Lambda}\text{Be}$ are not very different from ours, a dominant contribution from $2\pi/\sigma$ exchange to the $\Lambda\Lambda \rightarrow \Lambda n$ decay rate is obtained; this behavior is not confirmed by the chiral unitary approach based TPE mechanism adopted in the present study. The lack of details from [13] does not allow us to understand the origin of such a discrepancy. The ratio $\Gamma_{\Lambda n}/\Gamma_{\Sigma^0 n}$ is about 53 (49) for ${}^6_{\Lambda\Lambda}\text{He}$ (${}^{10}_{\Lambda\Lambda}\text{Be}$); both results are larger by about 80% than what is found in the present paper and in [12]. Furthermore, the ratio $\Gamma_n/\Gamma_{\Lambda n}$ is about 5.6 for ${}^6_{\Lambda\Lambda}\text{He}$, i.e., about 30% less than that found in the finite nucleus calculation of [12] for the same hypernucleus.

In [14] a hybrid quark-meson approach is instead adopted, which includes π - and K -exchange at long and medium distances and a direct quark mechanism (basically, a valence quark picture of baryons based on an effective four-quark weak Hamiltonian) to account for the short-range part of the processes. The direct quark mechanism provides a large contribution to the $\Gamma_{\Lambda n}$, $\Gamma_{\Sigma^0 n}$, and $\Gamma_{\Sigma^- p}$ decay rates and strongly violates the isospin rule of Eq. (12) (see the results in Table III). We note that the $\pi + K$ calculation provides $\Gamma_{\Lambda n}^K/\Gamma_{\Sigma^0 n}^\pi = 0.06$, in strong disagreement with the other calculations of Table III. We note that a simple evaluation in terms of the weak and strong coupling constants involved in the $\Lambda\Lambda \rightarrow \Lambda n$ decay mediated by the K meson and the $\Lambda\Lambda \rightarrow \Sigma^0 n$ decay mediated by the π meson indicates that the ratio $\Gamma_{\Lambda n}^K/\Gamma_{\Sigma^0 n}^\pi$ (which is a good approximation of the ratio $\Gamma_{\Lambda n}/\Gamma_{\Sigma^0 n}$; see the results of Table I) has to be larger than 1. When compared with the results of the present paper and of [12], the very small value of $\Gamma_{\Lambda n}^K/\Gamma_{\Sigma^0 n}^\pi$ originates from a “very small” K -exchange (“large” π -exchange) contribution to the $\Lambda\Lambda \rightarrow \Lambda n$ ($\Lambda\Lambda \rightarrow \Sigma^0 n$) channel. We point out the strong disagreement concerning K exchange: $\Gamma_{\Lambda n}^K/(10^{-2}\Gamma_{\Lambda n}^{\text{free}})$ is 0.03 in the hybrid quark-meson approach, while it is 1.7 (2.7) in the present approach (in the finite nucleus calculation of [12]). For the complete calculation, the hybrid quark-meson approach provides $\Gamma_{\Lambda n}/\Gamma_{\Sigma^0 n} \sim 0.37$.

As mentioned, no data is available on Λ -induced Λ decays, apart from the claim [10] for the detection of a single event in the KEK hybrid-emulsion experiment which led to the observation of the so-called NAGARA event consisting in the formation of the ${}^6_{\Lambda\Lambda}\text{He}$ hypernucleus. The authors interpreted this event as a weak decay of an unknown strangeness -2 system into a $\Sigma^- p$ pair. This result is difficult to interpret because the KEK experimental branching ratio (BR) for this process is of the order of 10^{-2} while for the $\Lambda\Lambda \rightarrow \Sigma^- p$

decay in a double- Λ hypernucleus the BR is evaluated to be of the order of 10^{-3} in the present work as well as in the previous determinations of [12,13]. As done in [10], one could also speculate that the observed event corresponds to a decay of an H dibaryon. As far as we know, there is only a dated calculation [27] concerning the $H \rightarrow \Sigma^- p$ process, which, adapted to the case of a double- Λ hypernucleus, provides a BR of the order of 10^{-2} . Future measurements will be essential not only to establish the Λ -induced Λ weak decays studied here but also to clarify the question of the existence and nature of the H dibaryon and eventually to establish its role in defining the properties of double- Λ hypernuclei. We conclude by mentioning that recent evidences have been obtained in lattice QCD calculations which point toward the existence of a bound H dibaryon [28,29]. These studies demonstrate that (small) hypernuclei could be directly treated with QCD in the future.

V. CONCLUSIONS

A microscopic diagrammatic approach is used to evaluate the nucleon- and Λ -induced Λ decay in double- Λ hypernuclei. The calculation is performed in nuclear matter and then extended to finite hypernuclei with mass numbers $A \sim 12$ (${}^{10}_{\Lambda\Lambda}\text{Be}$ and ${}^{13}_{\Lambda\Lambda}\text{B}$ are experimentally accessible cases) by means of the local density approximation. The present approach is the first one which takes into account the full one-meson-exchange weak transition potential together with two-pion-exchange contributions. The one-meson-exchange potential contains the mesons of the ground-state pseudoscalar and vector octets, while the two-pion-exchange potential includes correlated and uncorrelated terms and is obtained from the chiral unitary approach of [22,23]. Such a complete potential model proved to be of crucial importance in consistently explaining the whole set of decay data on single- Λ hypernuclei [1].

We confirm that the neutron- and proton-induced decay rates for the hypernucleus ${}^A_{\Lambda\Lambda}Z$ with $A \sim 12$ turn out to be larger (by about 5%) than twice the corresponding rates for the single- Λ hypernucleus ${}^{A-1}_{\Lambda}Z$; data indicate that the binding energy of a Λ is indeed larger in ${}^A_{\Lambda\Lambda}Z$ than in ${}^{A-1}_{\Lambda}Z$.

The two-pion-exchange mechanism turns out to provide a negligible contribution to the $\Lambda\Lambda \rightarrow \Lambda n$ nonmesonic decay of double- Λ hypernuclei. The rate $\Gamma_{\Lambda n}$ receives the major contributions from K and K^* exchange (however, the η meson cannot be neglected). The rates $\Gamma_{\Sigma^0 n}$ and $\Gamma_{\Sigma^- p}$, which are much smaller than $\Gamma_{\Lambda n}$ ($\Gamma_{\Lambda n}/\Gamma_{\Sigma^0 n} = 29$ and $\Gamma_{\Sigma^- p}/\Gamma_{\Sigma^0 n} = 2$ in virtue of the $\Delta I = 1/2$ isospin rule), are dominated by π exchange.

The total Λ -induced decay rate, $\Gamma_{\Lambda} = \Gamma_{\Lambda n} + \Gamma_{\Sigma^0 n} + \Gamma_{\Sigma^- p}$, amounts to about 1.2% of the total nonmesonic rate, $\Gamma_{\text{NM}} = \Gamma_n + \Gamma_p + \Gamma_2 + \Gamma_{\Lambda}$. We also find that the rate Γ_{Λ} decreases as the hypernuclear mass number A increases because the average distance between two Λ 's in a double- Λ hypernucleus is an increasing function of A .

Our final results for $\Gamma_{\Lambda n}$, $\Gamma_{\Sigma^0 n}$, and $\Gamma_{\Sigma^- p}$ are in fairly good agreement with the ones of [12,13] and in strong disagreement with those of [14].

We hope the present work may contribute to the start of a systematic investigation on the nonmesonic weak decays of

double- Λ hypernuclei. No reliable experimental evidence of interesting processes such as $\Lambda\Lambda \rightarrow \Lambda n$, $\Lambda\Lambda \rightarrow \Sigma^0 n$, and $\Lambda\Lambda \rightarrow \Sigma^- p$ is available at present. Future measurements will also be essential to clarify the question of the existence and nature of the H dibaryon and eventually to establish its interplay and/or mixing with the $\Lambda\Lambda$ pair in determining the structure and weak decays properties of double- Λ hypernuclei. New experimental programs at J-PARC and FAIR should thus be strongly supported.

ACKNOWLEDGMENTS

We would like to thank A. Ramos and A. Parreño for fruitful discussions. We are also grateful to T. Motoba for providing us with an eCopy of a publication by his group. This work was partially supported by the CONICET, Argentina, under Contract No. PIP 0032 and by the Agencia Nacional de Promociones Científicas y Técnicas, Argentina, under Contract No. PICT-2010-2688.

APPENDIX A

We present here the formal derivation of Eq. (4) which is used to calculate the decay rates in the local density approximation (LDA). Let us start by introducing the Λ pair wave function in coordinate space, $\psi_{\Lambda\Lambda}(\mathbf{r}, \mathbf{r}')$. In a double- Λ hypernucleus both hyperons are paired in the lowest energy $1s$ single-particle state. In the independent-particle approximation, $\psi_{\Lambda\Lambda}(\mathbf{r}, \mathbf{r}')$ is simply factorized in terms of the individual Λ wave functions $\psi_{\Lambda}(\mathbf{r})$ and $\psi_{\Lambda}(\mathbf{r}')$ associated with the same energy eigenvalue:

$$\psi_{\Lambda\Lambda}(\mathbf{r}, \mathbf{r}') = \psi_{\Lambda}(\mathbf{r})\psi_{\Lambda}(\mathbf{r}'). \quad (\text{A1})$$

Let us denote with \mathbf{k} and \mathbf{k}' (\mathbf{p}_1 and \mathbf{p}_2) the momenta of the initial Λ 's (final hyperon and nucleon) for the $\Lambda\Lambda \rightarrow YN$ decay. In the LDA one introduces the following rate for such a decay:

$$\Gamma_{YN}(\mathbf{k}) = \int d\mathbf{r} \int d\mathbf{r}' |\psi_{\Lambda\Lambda}(\mathbf{r}, \mathbf{r}')|^2 \Gamma_{YN}(\mathbf{k}, \mathbf{r}, \mathbf{r}'), \quad (\text{A2})$$

\mathbf{k} being the momentum of one of the initial Λ 's. The final momenta \mathbf{p}_1 and \mathbf{p}_2 are integrated out to obtain $\Gamma_{YN}(\mathbf{k}, \mathbf{r}, \mathbf{r}')$. Note also that momentum conservation, i.e., $\mathbf{k}' = \mathbf{p}_1 + \mathbf{p}_2 - \mathbf{k}$, implies that only one of the initial momenta (\mathbf{k}) is an independent variable once \mathbf{p}_1 and \mathbf{p}_2 are integrated out. This is the reason why the integrand in Eq. (A2) is independent of \mathbf{k}' .

The rates for finite hypernuclei are thus obtained through the relation:

$$\Gamma_{YN} = \int d\mathbf{k} |\tilde{\psi}_{\Lambda}(\mathbf{k})|^2 \Gamma_{YN}(\mathbf{k}), \quad (\text{A3})$$

$\tilde{\psi}_{\Lambda}(\mathbf{p})$ denoting the Fourier transform of $\psi_{\Lambda}(\mathbf{r})$.

Let us denote with \mathbf{r} the spatial point in which the final nucleon is created and with \mathbf{r}' the spatial point in which the initial Λ converts into the final hyperon. Then, introduce a local nucleon Fermi momentum depending on the position in which the final nucleon is created, $k_F(r) = \{3\pi^2 \rho(r)/2\}^{1/3}$, $\rho(r)$ being the density profile of the nuclear core. It follows that the function $\Gamma_{YN}(\mathbf{k}, \mathbf{r}, \mathbf{r}')$ is independent

of \mathbf{r}' and can be written as $\Gamma_{YN}(\mathbf{k}, k_F(r))$. Finally, from Eqs. (A1)–(A3) one simply obtains Eq. (4), which formally is the same relation used for the $\Lambda N \rightarrow nN$ nonmesonic decays.

APPENDIX B

The aim of this Appendix is twofold. First, we provide explicit expressions for the $\Lambda\Lambda \rightarrow \Lambda N$ and the $\Lambda\Lambda \rightarrow \Sigma N$ weak transition potentials as obtained through the exchange of the π , η , K , ρ , ω , and K^* mesons. Second, we briefly explain how to build up the general expression for the transition potential of Eq. (5) from these meson-exchange potentials.

Weak couplings are in units of $G_F m_\pi^2$ and are taken from [12]. The Nijmegen NSC97f model [30] is used for the strong coupling constants.

The $V^{\Lambda\Lambda \rightarrow \Lambda n}$ transition potential. This transition is of pure isoscalar nature ($\tau = 0$), thus the contributing mesons are η , ω , K , and K^* . We start with the η meson:

$$V_{\eta}(q) = G_F m_\pi^2 \frac{g_{\Lambda\Lambda\eta}}{2M} F_{\eta}^2(q) \times \left(A_{\eta} + \frac{B_{\eta}}{2\bar{M}} \boldsymbol{\sigma}_1 \cdot \mathbf{q} \right) \frac{\boldsymbol{\sigma}_2 \cdot \mathbf{q}}{q_0^2 - \mathbf{q}^2 - m_{\eta}^2}, \quad (\text{B1})$$

where $g_{\Lambda\Lambda\eta} = -6.56$, $A_{\eta} = 1.80$, $B_{\eta} = -11.9$, and $\Lambda_{\eta} = 1.75$ GeV and \bar{M} is the average between the nucleon and Λ masses.

For the ω meson we have

$$V_{\omega}(q) = G_F m_\pi^2 \left(g_{\Lambda\Lambda\omega}^V \alpha_{\omega} - \frac{(\alpha_{\omega} + \beta_{\omega})(g_{\Lambda\Lambda\omega}^V + g_{\Lambda\Lambda\omega}^T)}{4M\bar{M}} (\boldsymbol{\sigma}_1 \times \mathbf{q}) \cdot (\boldsymbol{\sigma}_2 \times \mathbf{q}) - i\varepsilon_{\omega} \frac{g_{\Lambda\Lambda\omega}^V + g_{\Lambda\Lambda\omega}^T}{2M} (\boldsymbol{\sigma}_1 \times \boldsymbol{\sigma}_2) \cdot \mathbf{q} \right) \frac{1}{q_0^2 - \mathbf{q}^2 - m_{\omega}^2}, \quad (\text{B2})$$

where $g_{\Lambda\Lambda\omega}^V = 7.11$, $g_{\Lambda\Lambda\omega}^T = -4.04$, $\alpha_{\omega} = -0.17$, $\beta_{\omega} = -7.43$, $\varepsilon_{\omega} = -1.33$, and $\Lambda_{\omega} = 1.31$ GeV.

Finally, we come to the isoscalar terms of the K and K^* exchange. The K -meson contribution reads (the isoscalar character of these terms is indicated by a $\tau = 0$ subindex)

$$V_{0,K}(q) = G_F m_\pi^2 \frac{g_{\Lambda\Lambda K}}{2M} F_K^2(q) \left(A_K + \frac{B_K}{2\bar{M}} \boldsymbol{\sigma}_1 \cdot \mathbf{q} \right) \times \frac{\boldsymbol{\sigma}_2 \cdot \mathbf{q}}{q_0^2 - \mathbf{q}^2 - m_K^2}, \quad (\text{B3})$$

with $g_{\Lambda\Lambda K} = -14.1$, $A_K = 0.67$, $B_K = 12.72$, $\Lambda_K = 1.8$ GeV, while for the K^* meson we have

$$V_{0,K^*}(q) = G_F m_\pi^2 \left(g_{\Lambda\Lambda K^*}^V \alpha_{K^*} - \frac{(\alpha_{K^*} + \beta_{K^*})(g_{\Lambda\Lambda K^*}^V + g_{\Lambda\Lambda K^*}^T)}{4M\bar{M}} (\boldsymbol{\sigma}_1 \times \mathbf{q}) \cdot (\boldsymbol{\sigma}_2 \times \mathbf{q}) \right)$$

$$\begin{aligned}
 & -i\varepsilon_{K^*} \frac{g_{\Lambda N K^*}^V + g_{\Lambda N K^*}^T}{2M} (\boldsymbol{\sigma}_1 \times \boldsymbol{\sigma}_2) \cdot \mathbf{q} \\
 & \times \frac{1}{q_0^2 - \mathbf{q}^2 - m_{K^*}^2}, \quad (\text{B4})
 \end{aligned}$$

where $g_{\Lambda N K^*}^V = -5.47$, $g_{\Lambda N K^*}^T = -11.9$, $\alpha_{K^*} = -1.34$, $\beta_{K^*} = 11.2$, $\varepsilon_{K^*} = -1.38$, and $\Lambda_{K^*} = 1.65$ GeV.

The $V^{\Lambda\Lambda \rightarrow \Sigma^0 n}$ transition potential. This transition is of pure isovector nature ($\tau = 1$), thus the contributing mesons are π , ρ , K , and K^* . We begin with the π meson:

$$\begin{aligned}
 V_\pi(q) &= G_F m_\pi^2 \frac{g_{\Lambda\Sigma\pi}}{2M} F_\pi^2(q) \left(A_\pi + \frac{B_\pi}{2M} \boldsymbol{\sigma}_1 \cdot \mathbf{q} \right) \\
 & \times \frac{\boldsymbol{\sigma}_2 \cdot \mathbf{q} \boldsymbol{\tau}_1 \cdot \boldsymbol{\tau}_2}{q_0^2 - \mathbf{q}^2 - m_\pi^2}, \quad (\text{B5})
 \end{aligned}$$

where $g_{\Lambda\Sigma\pi} = 12.0$, $A_\pi = -1.05$, $B_\pi = 7.15$, and $\Lambda_\pi = 1.75$ GeV.

For the ρ meson we have

$$\begin{aligned}
 V_\rho(q) &= G_F m_\pi^2 \left(g_{\Lambda\Sigma\rho}^V \alpha_\rho - \frac{(\alpha_\rho + \beta_\rho)(g_{\Lambda\Sigma\omega}^V + g_{\Lambda\Sigma\rho}^T)}{4M\bar{M}} \right) \\
 & \times (\boldsymbol{\sigma}_1 \times \mathbf{q}) \cdot (\boldsymbol{\sigma}_2 \times \mathbf{q}) \\
 & - i\varepsilon_\rho \frac{g_{\Lambda\Sigma\rho}^V + g_{\Lambda\Sigma\rho}^T}{2M} (\boldsymbol{\sigma}_1 \times \boldsymbol{\sigma}_2) \cdot \mathbf{q} \frac{\boldsymbol{\tau}_1 \cdot \boldsymbol{\tau}_2}{q_0^2 - \mathbf{q}^2 - m_\rho^2}, \quad (\text{B6})
 \end{aligned}$$

where $g_{\Lambda\Sigma\rho}^V = 0.0$, $g_{\Lambda\Sigma\rho}^T = 11.2$, $\alpha_\rho = 3.29$, $\beta_\rho = 6.74$, $\varepsilon_\rho = -1.09$, and $\Lambda_\rho = 1.23$ GeV.

Finally, we come to the isovector terms of the K and K^* exchange. The K -meson contribution reads (the $\tau = 1$ subindex indicates the isovector character of the interaction)

$$\begin{aligned}
 V_{1,K}(q) &= G_F m_\pi^2 \frac{g_{\Lambda N K}}{2M} F_K^2(q) \left(\tilde{A}_K + \frac{\tilde{B}_K}{2M} \boldsymbol{\sigma}_1 \cdot \mathbf{q} \right) \\
 & \times \frac{\boldsymbol{\sigma}_2 \cdot \mathbf{q} \boldsymbol{\tau}_1 \cdot \boldsymbol{\tau}_2}{q_0^2 - \mathbf{q}^2 - m_K^2}, \quad (\text{B7})
 \end{aligned}$$

with $g_{\Lambda N K} = -14.1$, $\tilde{A}_K = 0.39$, $\tilde{B}_K = 5.95$, $\Lambda_K = 1.8$ GeV, while for the K^* meson we have

$$\begin{aligned}
 V_{1,K^*}(q) &= G_F m_\pi^2 \left(g_{\Lambda N K^*}^V \tilde{\alpha}_{K^*} \right. \\
 & - \frac{(\tilde{\alpha}_{K^*} + \tilde{\beta}_{K^*})(g_{\Lambda N K^*}^V + g_{\Lambda N K^*}^T)}{4M\bar{M}} (\boldsymbol{\sigma}_1 \times \mathbf{q}) \cdot (\boldsymbol{\sigma}_2 \times \mathbf{q}) \\
 & - i\tilde{\varepsilon}_{K^*} \frac{g_{\Lambda N K^*}^V + g_{\Lambda N K^*}^T}{2M} (\boldsymbol{\sigma}_1 \times \boldsymbol{\sigma}_2) \cdot \mathbf{q} \left. \right) \\
 & \times \frac{\boldsymbol{\tau}_1 \cdot \boldsymbol{\tau}_2}{q_0^2 - \mathbf{q}^2 - m_{K^*}^2}, \quad (\text{B8})
 \end{aligned}$$

where $g_{\Lambda N K^*}^V = -5.47$, $g_{\Lambda N K^*}^T = -11.9$, $\tilde{\alpha}_{K^*} = -3.9$, $\tilde{\beta}_{K^*} = 4.45$, $\tilde{\varepsilon}_{K^*} = 0.63$, and $\Lambda_{K^*} = 1.65$ GeV.

To obtain the transition potential of Eq. (5), first short-range correlations (SRC) have to be implemented. The procedure to do this is explained in Appendix B of [20] for the $V^{\Lambda N \rightarrow n N}$ transition potential. Once this is done, it is very simple to

identify the expressions for the functions $S_\tau(q)$, $S'_\tau(q)$, $P_{L,\tau}(q)$, $P_{C,\tau}(q)$, $P_{T,\tau}(q)$, and $S_{V,\tau}(q)$ entering Eqs. (5) and (6). Just as an example, by neglecting SRC and considering only the π -meson transition potential of Eq. (B5), it is straightforward to identify the parity-violating term of this potential with a contribution to $S_{\tau=1}(q)$ and the parity-conserving term with $P_{L,\tau=1}(q)$.

The explicit expressions for the functions $S_\tau(q)$, $S'_\tau(q)$, $P_{L,\tau}(q)$, $P_{C,\tau}(q)$, $P_{T,\tau}(q)$, and $S_{V,\tau}(q)$ entering in the potential $V^{\Lambda\Lambda \rightarrow Y N}$ are obtained from the ones corresponding to $V^{\Lambda N \rightarrow n N}$ as follows: (i) The $V^{\Lambda\Lambda \rightarrow \Lambda n}$ potential, which is isoscalar, is obtained by making the following replacements for the strong coupling constants, $g_{NN\eta} \rightarrow g_{\Lambda\Lambda\eta}$, $g_{NN\omega}^V \rightarrow g_{\Lambda\Lambda\omega}^V$, $g_{NN\omega}^T \rightarrow g_{\Lambda\Lambda\omega}^T$. Analogously, the NNK and NNK^* weak parity-conserving and parity-violating coupling constants are replaced by the $\Lambda\Lambda K$ and $\Lambda\Lambda K^*$ couplings, respectively; (ii) for the $V^{\Lambda\Lambda \rightarrow \Sigma^0 n}$ potential, which is isovector, the following replacements have to be made—for the strong coupling constants, $g_{NN\pi} \rightarrow g_{\Lambda\Sigma\pi}$, $g_{NN\rho}^V \rightarrow g_{\Lambda\Sigma\rho}^V$, and $g_{NN\rho}^T \rightarrow g_{\Lambda\Sigma\rho}^T$; the NNK and NNK^* weak coupling constants are replaced by the $\Lambda\Sigma K$ and $\Lambda\Sigma K^*$ couplings, respectively.

APPENDIX C

In this Appendix we present expressions for the evaluation of $\Gamma_{\Sigma^0 n}$ and $\Gamma_{\Sigma^- p}$. Note that, as explained in the text, by neglecting the small mass difference between the Σ^0 and Σ^- hyperons, the enforcement of the $\Delta I = 1/2$ isospin rule leads to $\Gamma_{\Sigma^- p} = 2\Gamma_{\Sigma^0 n}$.

For $\Gamma_{\Sigma^0 n} = -2 \text{Im} \Sigma_{\Sigma^0 n}$ we have

$$\begin{aligned}
 \Gamma_{\Sigma^0 n}(\mathbf{k}, k_F) &= -2 \text{Im} \int \frac{d^4 p_1}{(2\pi)^4} \int \frac{d^4 p_2}{(2\pi)^4} G_{\Sigma^0}(p_1) G_n(p_2) \frac{1}{4} \\
 & \times \sum_{\text{all spins}} \langle \gamma_{\Lambda(k)} \gamma_{\Lambda(k')} | (V^{\Lambda\Lambda \rightarrow \Sigma^0 n})^\dagger | \gamma_{\Sigma^0(p_1)} \gamma_{n(p_2)} \rangle_{\text{ant}} \\
 & \times \langle \gamma_{\Sigma^0(p_1)} \gamma_{n(p_2)} | V^{\Lambda\Lambda \rightarrow \Sigma^0 n} | \gamma_{\Lambda(k)} \gamma_{\Lambda(k')} \rangle_{\text{ant}}, \quad (\text{C1})
 \end{aligned}$$

where with $\gamma_{B(K)}$ we represent the spin, isospin, and energy-momentum K , of the baryon B . The Λ , Σ , and neutron propagators read

$$G_\Lambda(p) = \frac{1}{p_0 - E_\Lambda(\mathbf{p}) - V_\Lambda + i\varepsilon}, \quad (\text{C2})$$

$$G_\Sigma(p) = \frac{1}{p_0 - E_\Sigma(\mathbf{p}) - V_\Sigma + i\varepsilon}, \quad (\text{C3})$$

and

$$G_N(p) = \frac{\theta(|\mathbf{p}| - k_F)}{p_0 - E_N(\mathbf{p}) - V_N + i\varepsilon}, \quad (\text{C4})$$

respectively, V_Λ , V_Σ , and V_N representing binding energies. After performing the summation over spin, the evaluation of the isospin matrix element and the energy integration, one obtains the antisymmetrized $\Lambda\Lambda \rightarrow \Sigma^0 n$ decay rate in nuclear matter as

$$\Gamma_{\Sigma^0 n}(\mathbf{k}, k_F) = \frac{\pi}{3} (G_F m_\pi^2)^2 \int \frac{d^3 p_1}{(2\pi)^3} \int \frac{d^3 p_2}{(2\pi)^3} (2\mathcal{W}_1^{\text{dir}}(q) - \mathcal{W}_1^{\text{exch}}(q, Q)) \times \theta(|\mathbf{p}_2| - k_F) \delta(k_0 + k'_0 - E_{\Sigma^0}(p_1) - E_n(p_2)), \quad (\text{C5})$$

where E_Λ (E_n) is the total Λ (neutron) energy. For the direct and exchange terms, the momentum matrix elements of the interaction turn out to be

$$\mathcal{W}_1^{\text{dir}}(q) = \{S_1^2(q) + S_1'^2(q) + P_{L,1}^2(q) + P_{C,1}^2(q) + 2P_{T,1}^2(q) + 2S_{V,1}^2(q)\}, \quad (\text{C6})$$

and

$$\begin{aligned} \mathcal{W}_1^{\text{exch}}(q, Q) = & (\hat{\mathbf{q}} \cdot \hat{\mathbf{Q}}) \mathcal{S}_1(q, Q) + (2(\hat{\mathbf{q}} \cdot \hat{\mathbf{Q}})^2 - 1) P_{L,1}(q) P_{L,1}(Q) + 2((\hat{\mathbf{q}} \cdot \hat{\mathbf{Q}})^2 - 1) P_{T,1}(q) P_{T,1}(Q) \\ & - 2(\hat{\mathbf{q}} \cdot \hat{\mathbf{Q}})^2 (P_{L,1}(q) P_{T,1}(Q) + P_{L,1}(Q) P_{T,1}(q)) + P_{C,1}(q) P_{C,1}(Q) + P_{C,1}(q) P_{L,1}(Q) + P_{C,1}(Q) P_{L,1}(q) \\ & + 2(P_{C,1}(q) P_{T,1}(Q) + P_{C,1}(Q) P_{T,1}(q)), \end{aligned} \quad (\text{C7})$$

respectively, where $q = k - p_1$, $Q = k - p_2$, and

$$\mathcal{S}_1(q, Q) = (S_1(q) + S_1'(q))(S_1(Q) + S_1'(Q)) - 2(S_1(q)S_{V,1}(Q) + S_{V,1}(q)S_1(Q)) + 2(S_1'(q)S_{V,1}(Q) + S_{V,1}(q)S_1'(Q)). \quad (\text{C8})$$

The finite hypernucleus decay rate $\Gamma_{\Sigma^0 n}$ is then obtained by means of the LDA of Eq. (4).

-
- [1] E. Botta, T. Bressani, and G. Garbarino, *Eur. Phys. J. A* **48**, 41 (2012); S. Bufalino, *Nucl. Phys. A* **914**, 160 (2013); H. Outa, in *Hadron Physics*, Proceedings of the International School of Physics ‘‘E. Fermi’’ Course CLVIII, edited by T. Bressani, A. Filippi, and U. Wiedner (IOS Press, Amsterdam, 2005), p. 21; W. M. Alberico and G. Garbarino, *Phys. Rep.* **369**, 1 (2002).
- [2] E. Bauer, G. Garbarino, A. Parreno, and A. Ramos, *Nucl. Phys. A* **836**, 199 (2010).
- [3] E. Bauer and G. Garbarino, *Phys. Lett. B* **698**, 306 (2011).
- [4] E. Bauer and G. Garbarino, *Phys. Lett. B* **716**, 249 (2012).
- [5] K. Nakazawa and H. Takahashi, *Prog. Theor. Phys. Suppl.* **185**, 335 (2010).
- [6] J. K. Ahn *et al.*, *Phys. Rev. C* **88**, 014003 (2013); H. Takahashi *et al.*, *Phys. Rev. Lett.* **87**, 212502 (2001).
- [7] A. Gal and D. J. Millener, *Phys. Lett. B* **701**, 342 (2011); *Hyperfine Interact.* **210**, 77 (2012).
- [8] T. Takahashi, *Nucl. Phys. A* **914**, 530 (2013).
- [9] A. Sanchez Lorente *et al.*, *Hyperfine Interact.* **229**, 45 (2014); U. Wiedner, *Prog. Part. Nucl. Phys.* **66**, 477 (2011).
- [10] T. Watanabe *et al.*, *Eur. Phys. J. A* **33**, 265 (2007).
- [11] R. L. Jaffe, *Phys. Rev. Lett.* **38**, 195 (1977); **38**, 617 (1977).
- [12] A. Parreño, A. Ramos, and C. Bennhold, *Phys. Rev. C* **65**, 015205 (2001).
- [13] K. Itonaga, T. Ueda, and T. Motoba, *Nucl. Phys. A* **691**, 197c (2001); *Mod. Phys. Lett. A* **18**, 135 (2003).
- [14] K. Sasaki, T. Inoue, and M. Oka, *Nucl. Phys. A* **726**, 349 (2003).
- [15] E. Bauer and G. Garbarino, *Nucl. Phys. A* **828**, 29 (2009).
- [16] E. Bauer and G. Garbarino, *Phys. Rev. C* **81**, 064315 (2010).
- [17] E. Bauer, G. Garbarino, A. Parreño, and A. Ramos, *Phys. Rev. C* **85**, 024321 (2012).
- [18] E. Oset and L. L. Salcedo, *Nucl. Phys. A* **443**, 704 (1985).
- [19] J. Caro, C. Garcia-Recio, and J. Nieves, *Nucl. Phys. A* **646**, 299 (1999).
- [20] E. Bauer and F. Krmpotić, *Nucl. Phys. A* **717**, 217 (2003).
- [21] C. Chumillas, G. Garbarino, A. Parreno, and A. Ramos, *Phys. Lett. B* **657**, 180 (2007).
- [22] D. Jido, E. Oset, and J. E. Palomar, *Nucl. Phys. A* **694**, 525 (2001).
- [23] K. Sasaki, E. Oset, and M. J. Vicente Vacas, *Phys. Rev. C* **74**, 064002 (2006); *Eur. Phys. J. A* **31**, 557 (2007).
- [24] A. Pérez-Obiol, D. R. Entem, B. Juliá-Díaz, and A. Parreño, *Phys. Rev. C* **87**, 044614 (2013).
- [25] Note that available experimental values of the harmonic oscillator parameter $\hbar\omega$ (obtained as the energy separation between the s and p Λ -levels) are -10.8 MeV for ^{12}C and -13.6 MeV for $A = 6-13$ double- Λ hypernuclei.
- [26] K. Itonaga, T. Ueda, and T. Motoba, *Phys. Rev. C* **65**, 034617 (2002).
- [27] J. F. Donoghue, E. Golowich, and B. R. Holstein, *Phys. Rev. D* **34**, 3434 (1986).
- [28] S. R. Beane *et al.* (PLQCD Collaboration), *Phys. Rev. Lett.* **106**, 162001 (2011).
- [29] T. Inoue *et al.* (HAL QCD Collaboration), *Phys. Rev. Lett.* **106**, 162002 (2011).
- [30] V. G. J. Stoks and Th. A. Rijken, *Phys. Rev. C* **59**, 3009 (1999); Th. A. Rijken, V. G. J. Stoks, and Y. Yamamoto, *ibid.* **59**, 21 (1999).